RESEARCH ARTICLE

Key Points:
- The new type of explosively growing vortices in unstably stratified atmosphere is investigated
- The results obtained are in a good agreement with existing observations and laboratory experiments
- It is shown that in our model the vertical vorticity and toroidal speed exponentially increase in time

Correspondence to:
V. Fedun,
v.fedun@sheffield.ac.uk

"Explosively growing" vortices of unstably stratified atmosphere

O. G. Onishchenko[1,2], W. Horton[3], O. A. Pokhotelov[1], and V. Fedun[4]

[1]Institute of Physics of the Earth, Moscow, Russia, [2]Space Research Institute, Moscow, Russia, [3]Department of Physics and Institute for Fusion Studies, University of Texas at Austin, Austin, Texas, USA, [4]Department of Automatic Control and Systems Engineering, University of Sheffield, Sheffield, UK

Abstract A new type of "explosively growing" vortex structure is investigated theoretically in the framework of ideal fluid hydrodynamics. It is shown that vortex structures may arise in convectively unstable atmospheric layers containing background vorticity. From an exact analytical vortex solution the vertical vorticity structure and toroidal speed are derived and analyzed. The assumption that vorticity is constant with height leads to a solution that grows explosively when the flow is inviscid. The results shown are in agreement with observations and laboratory experiments

1. Introduction

Dust devils and tornadoes are regular phenomena in the Earth's atmosphere. In fair weather dust devils form in the atmospheric boundary layer but tornadoes develop in thunderstorm clouds. Although they appear under different conditions, these phenomena can be collectively described as "concentrated vortices" [see, e.g., *Mullen and Maxworthy*, 1977; *Church et al.*, 1979; *Rennó and Bluestein*, 2001; *Ringrose*, 2005; *Balme and Greeley*, 2006]. Due to the lower atmospheric pressure, in comparison with Earth, dust devils in the Martian atmosphere can develop into larger structures. Observations of dust devils have been reported by a number of authors, i.e., *Metzger et al.* [1999], *Thomas and Gierasch* [1985], *Ferri et al.* [2003], *Kanak* [2006], *Greeley et al.* [2010], and *Nishizawa et al.* [2016]. These observations show that vortex structures have toroidal speeds of the order of 10 m/s, in the case of dust devils, and of the order of 100 m/s in tornadoes [see, e.g., *Mullen and Maxworthy*, 1977; *Church et al.*, 1979; *Hess and Spillane*, 1990; *Balme and Greeley*, 2006]. Concentrated vortices are relatively short-scale structures with characteristic perpendicular scales stretching from a meter up to a few hundred meters which are elongated in the vertical direction. Their lifetimes range from a few minutes to a few hours. Also, rotational and vertical wind speeds of vortices are positively correlated with their size [see, e.g., *Ryan and Carroll*, 1970]. Observations, numerical simulations, and laboratory experiments show that in the internal region of a vortex, the toroidal velocity increases with the radial distance from zero up to maximum at the vortex radius r_0. In the external region the approximate decrease in velocity is inversely proportional to the radial distance; hence, the Rankine model is often used to interpret the observations of concentrated vortices [see, e.g., *Balme and Greeley*, 2006]. The flow field of the Rankine model only has a toroidal velocity component, which depends solely on the radial distance from the vortex center with the maximum velocity attained at the vortex radius. Unlike the Rankine vortex, the Burgers vortex has a dependence on both the radial and vertical flow [see, e.g., *Burgers*, 1948]. This vortex corresponds to the exact solution to the Navier-Stokes equations governing viscous flow. For the Burgers model an inward radial flow develops that concentrates the vertical vorticity in a narrow column around the symmetry axis. As a model of a real dust devil or tornado, the Rankine and Burgers vortices both have their deficiencies. These models describe vortices in a stationary state, while the actual time-dependent mechanism of their generation remains unclear. The dust devil's potential intensity has been estimated in the framework of the simple thermodynamic theory developed by *Rennó et al.* [1998]. In a stably stratified atmosphere dust devil's dynamics were studied analytically and numerically by *Horton et al.* [2016]. These authors also investigated the influence that air viscosity has on the formation of vortex structures. The lifetime of such vortices can be divided into three stages: initial formation or generation, existence in the quasi-stationary state, and dissipation. The formation time is substantially smaller when compared to the vortex lifetime. According to observations reported by *Balme and Greeley* [2006] and *Sinclair* [1973], the lower part of the "typical" dust devil can be described as an "inverted cone whose apex is touching or near to the ground," which tends to a cylindrical shape at a higher altitude.

Onishchenko et al. [2015] studied the lower V-shaped vertical vorticity of dust devils and developed a reduced nonlinear model of vortex generation for a narrow central region when $r/r_0 \ll 1$ or $r/r_0 \gg 1$, where r_0 is the vortex radius.

In this paper, we generalize the theory for finite r/r_0 and show that these vortices exhibit "explosive growth." The effect of amplitude saturation can be explained by energy dissipation, longitudinal temperature gradients, and the influence of dust on the instability growth rate. However, this analysis is out of scope of the present study and will be the subject of future research.

The paper is organized as follows. In the first part of section 2 we describe the nonlinear model which has been used for vortex structure analysis. In the second part of section 2 we obtain the expressions for radial and vertical velocity components of the generated convective motion. Using these expressions we investigate the generation of the vertical vorticity and toroidal velocity. Section 3 contains final comments and conclusions.

2. The Nonlinear Model

In cylindrical coordinates (r, ϕ, z) we only consider the axisymmetric case with $\partial/\partial\phi = 0$. We also neglect the influence of dissipative processes such as viscosity, friction, thermal conductivity, and heat flows. The most general divergence-free flow velocity $\mathbf{v}$ can be decomposed into its poloidal $\mathbf{v}_\perp = (v_r, 0, v_z)$ and toroidal $v_\phi(r)\hat{\mathbf{e}}_\phi$ parts, i.e., $\mathbf{v} = \mathbf{v}_\perp + v_\phi\hat{\mathbf{e}}_\phi$, where $\mathbf{v}_\perp = \nabla \times (\psi \times \nabla\phi) = \nabla\psi \times \nabla\phi$. Here $\psi(t, r, z)$ is the stream function:

$$v_r = -\frac{1}{r}\frac{\partial\psi}{\partial z}, \quad v_z = \frac{1}{r}\frac{\partial\psi}{\partial r}. \tag{1}$$

From *Onishchenko et al.* [2014] the ideal fluid equation describing nonlinear internal gravity waves is

$$\left(\frac{\partial^2}{\partial t^2} + \omega_g^2\right)\Delta^*\psi + \frac{1}{r}\frac{\partial}{\partial t}J(\psi, \Delta^*\psi) = 0, \tag{2}$$

where ω_g stands for the Brunt-Väisälä or buoyancy frequency

$$\omega_g^2 = g\left(\frac{1}{T}\frac{dT}{dz} + \frac{\gamma_a - 1}{\gamma_a H}\right) \tag{3}$$

and

$$\Delta^* = r\frac{\partial}{\partial r}\frac{1}{r}\frac{\partial}{\partial r} + \frac{\partial^2}{\partial z^2}. \tag{4}$$

Here $J(A, B) = (\partial A/\partial r)\partial B/\partial z - (\partial A/\partial z)\partial B/\partial r$ is the Jacobian, γ_a is the ratio of specific heats, H is the reduced height of atmosphere, g is the gravity acceleration, and T is the temperature. Equation (2) can also be obtained from the system of two equations originally derived by *Stenflo* [1996] and has been discussed recently by *Shukla and Stenflo* [2012] and *Onishchenko et al.* [2013]. This equation describes the dynamics of convective motion in an unstable atmosphere, when $\omega_g^2 < 0$ [*Onishchenko et al.*, 2014, 2015]. Using the approximation $\partial\omega_z/\partial z = 0$, where $\omega_z = (\nabla \times \mathbf{v})_z$, the interaction of the growing convective motion with vertical vorticity ω_z is described by the equation

$$\frac{\partial\omega_z}{\partial t} + v_r\frac{\partial\omega_z}{\partial r} = \omega_z\frac{\partial v_z}{\partial z}. \tag{5}$$

Here the second term on the left-hand side and the term on the right-hand side give rise to a stretching of vortex lines which has the effect of intensifying vorticity. According to Kelvin's theorem, the total circulation of the vortex lines has to be constant, and thus, the axial stretching of vorticity lines increases their vorticity.

Nonlinear equations (2) and (5), with the use of equation (1), describe a generation of vortex structures in the stratified atmosphere. Here we are looking for an ω_z solution with toroidal velocity v_ϕ bounded in the perpendicular direction. The stream function we use is
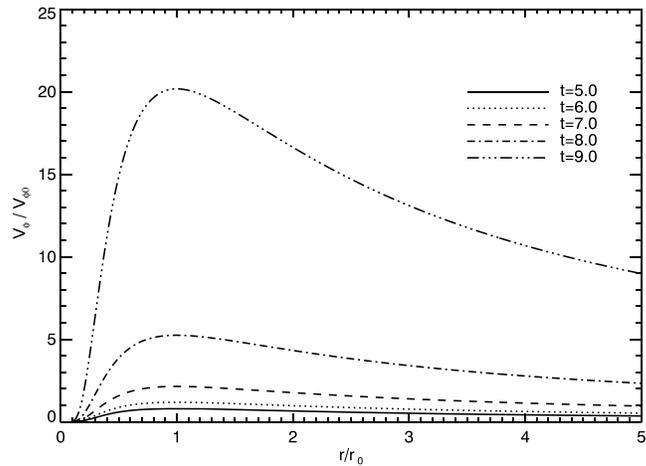
$$\psi = r_0^2\Psi(R, z)\exp(\gamma t), \tag{6}$$

Figure 1. The normalized toroidal velocity $v_\phi/v_{\phi 0}$ (see equation (13)) as a function of dimensionless radius r/r_0. For this case $\alpha/\gamma = 0.1$ and $\gamma = 0.41$.

where $R = r/r_0$, r_0 is the vortex radius and γ stands for the constant growth rate. Assuming

$$\Psi = \alpha z R^3, \tag{7}$$

we obtain:

$$\Delta^* \Psi = 3\alpha z \frac{R}{r_0^2} \tag{8}$$

By taking into account $(\alpha/\gamma) R \ll 1$, in the linear approximation from equation (2) for unstable stratification we obtain $\gamma = |\omega_g|$. The radial and vertical velocity components are

$$v_r = -\alpha r_0 R^2 \exp(\gamma t) \tag{9}$$

and

$$v_z = 3\alpha z R \exp(\gamma t), \tag{10}$$

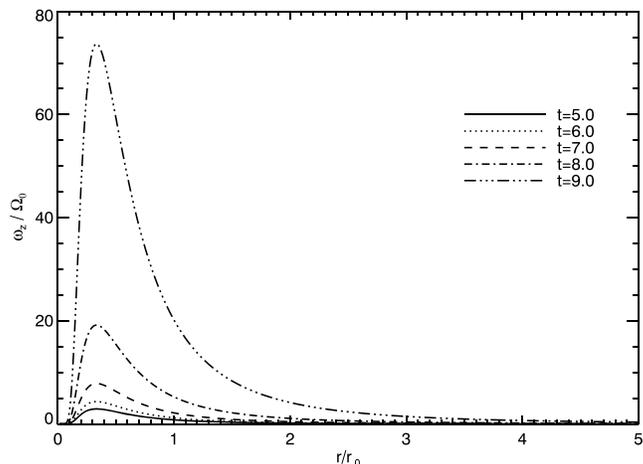where $\alpha > 0$ is a constant value describing the strength of suction into the vortex.

Figure 2. The normalized vertical component of vorticity ω_z/Ω_0 (see equation (13)) as a function of radius r/r_0. For this case α/γ is equal 0.1 and $\gamma = 0.41$, respectively.
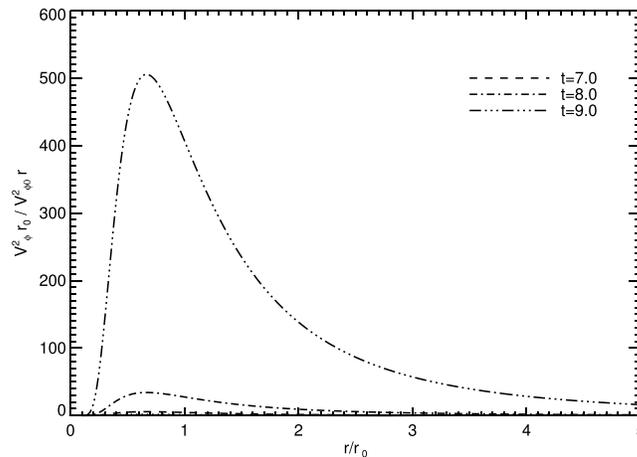
Figure 3. The normalized value of $r_0 v_\phi^2/v_{\phi 0}^2 r$ as a function of r/r_0. Here α/γ is equal 0.1. The values of $r_0 v_\phi^2/v_{\phi 0}^2 r$ for $t = 5.0$ and 6.0 are small and not shown on the plot.

The stream lines of the vortex are concentric circles given by $dz/dr = v_z/v_r$. Making use of equations (9) and (10), we obtain the following expressions for the particle trajectories in the internal and external regions $zr^3 = \text{const}$. The poloidal vorticity determined by $\omega_\phi = -\partial v_z/\partial r$ is

$$\omega_\phi = -3\alpha\left(z/r_0\right)\exp(\gamma t). \tag{11}$$

It is seen that ω_ϕ is always negative. Now we turn to the solution of equation (5) in the presence of an external background vertical vorticity which we represent in a simple one-parametric form of spatially localized vortex $\Omega_z = \Omega\left[1 - \exp\left(-r^2/a^2\right)\right]$ with a characteristic spatial scale $a \gg r_0$ and maximum vorticity Ω when $r = a$. We use this representation as an initial stage of the vertical vorticity $\omega_z(0, r) = \Omega r^2/a^2$, where $\Omega = \text{const}$. After substituting equations (9) and (10) into equation (5), we find that

$$\frac{\omega_z}{\Omega_0} = \frac{1}{R^5}\exp\left(\frac{\alpha}{\gamma}\exp(\gamma t) - \frac{1}{R}\right), \tag{12}$$

where $\Omega_0 = \Omega(r_0^2/a^2)$ is the background vertical vorticity at $r = r_0$. The double exponential term in equation (12) describes the explosively growing dependence of the ω_z. The vertical vorticity attains the maximum value when $R = 1/3$, and signs of ω_z and Ω coincide. Making use of equation (12) and relation $r\omega_z = \partial(rv_\phi)/\partial r$ one obtains the toroidal velocity v_ϕ in the form

$$\frac{v_\phi}{v_{\phi 0}} = \frac{1}{R}\exp\left(\frac{\alpha}{\gamma}\exp(\gamma t) - \frac{1}{R}\right), \tag{13}$$

where $v_{\phi 0} = \Omega r_0(r_0^2/4a^2)$ is the background toroidal velocity at $r = r_0$. The toroidal speed attains the maximum value $v_\phi/v_{\phi 0} = \exp\left(\frac{\alpha}{\gamma}\exp(\gamma t) - 1\right)$ at $R = 1$. The vertical vorticity and toroidal velocity shown in equations (12) and (13), respectively, are proportional to the double exponential function. This corresponds to the explosive growth of the vortex structure. Similar to the Burgers and Rankine vortices [see, e.g., *Burgers*, 1948; *Balme and Greeley*, 2006], the toroidal velocity v_ϕ is proportional to $1/r$ for large values of R.

3. Conclusions

In the framework of ideal hydrodynamics, we obtained a new exact solution which describes the explosive growth of vortex structures in the Earth, planetary and under some restrictions even in the solar atmosphere. Convective instabilities present in the atmosphere layer, along with background vorticity, are necessary conditions for this rapid vortex formation. Similar to Burgers's vortex model, the vertical and radial components of the flow (see equations (9) and (10)) depend on the parameter α, which characterizes the strength of suction into the vortex. The toroidal velocity distribution for $r \gg r_0$ decreases as an inverse function of radius in accordance with laboratory observations [see, e.g., *Balme and Greeley*, 2006; *Mullen and Maxworthy*, 1977],

as well as in the models by Rankine and Burgers. From equations (12) and (13) it is seen that vertical vorticity ω_z and toroidal velocity v_ϕ are independent of z. After a moderate time, i.e., $t > \gamma^{-1}$, the amplification factor shows an anomalously strong character if $(\alpha/\gamma) \exp(\gamma t) > 1$. For a numerical calculation, we use the temperature lapse rate 2°C m^{-1} [see, e.g., *Oke et al.*, 2007] which results in a convective instability growth rate of $\gamma = 0.25$ s^{-1}. Figures 1 and 2 show the dependence of normalized vertical vorticity and toroidal velocities in a vortex within the time interval $5 \leq t \leq 9$ s when $\alpha = 0.1\gamma$.

Taking into account the radial dependance of the toroidal velocity v_ϕ for different times, one can calculate the pressure gradient $\partial p/\partial r = \rho v_\phi^2/r$, where p and ρ are the pressure and mass density, respectively. Figure 3 shows the time evolution of the normalized pressure gradient versus r/r_0. It should be noted that this model of vortex generation is applicable to tornadoes or dust devil vortices with a single-celled structure [e.g., *Balme and Greeley*, 2006] and can also be used for the investigation of acoustic-gravity tornadoes [e.g., *Shukla and Stenflo*, 2012].

References

Balme, M., and R. Greeley (2006), Dust devils on Earth and Mars, *Rev. Geophys.*, *44*, RG3003, doi:10.1029/2005RG000188.

Burgers, J. M. (1948), A mathematical model illustrating the theory of turbulence, *Adv. Appl. Mech.*, *1*, 171–199.

Church, C. R., G. L. Baker, and E. M. Agee (1979), Characteristics of tornado-like vortices as a function of swirl ratio: A laboratory investigation, *J. Atmos. Sci.*, *36*(9), 1755–1776.

Ferri, F., P. H. Smith, M. Lemmon, and N. O. Rennó (2003), Dust devils as observed by Mars Pathfinder, *J. Geophys. Res.*, *108*(E12), 5133, doi:10.1029/2000JE001421.

Greeley, R., D. A. Waller, N. A. Cabrol, G. A. Landis, M. T. Lemmon, L. D. V. Neakrase, M. Pendleton Hoffer, S. D. Thompson, and P. L. Whelley (2010), Gusev Crater, Mars: Observations of three dust devil seasons, *J. Geophys. Res.*, *115*, E00F02, doi:10.1029/2010JE003608.

Hess, G. D., and K. T. Spillane (1990), Characteristics of dust devils in Australia, *J. Appl. Meteorol.*, *29*, 498–507.

Horton, W., H. Miura, O. Onishchenko, L. Couedel, C. Arnas, A. Escarguel, S. Benkadda, and V. Fedun (2016), Dust devil dynamics, *J. Geophys. Res. Atmos.*, *121*, 7197–7214, doi:10.1002/2016JD024832.

Kanak, K. M. (2006), On the numerical simulation of dust devil-like vortices in terrestrial and Martian convective boundary layer, *Geophys. Res. Lett.*, *33*, L19S05, doi:10.1029/2006GL026207.

Metzger, S. M., J. R. Carr, J. R. Johnson, T. J. Parker, and M. T. Lemmon (1999), Dust devil vortices seen by the Mars Pathfinder camera, *Geophys. Res. Lett.*, *26*(18), 2781–2784.

Mullen, J. B., and T. A. Maxworthy (1977), A laboratory model of dust devil vortices, *Dyn. Atmos. Ocean*, *1*(3), 181–214.

Nishizawa, S., et al. (2016), Martian dust devil statistics from high-resolution large-eddy simulations, *Geophys. Res. Lett.*, *43*, 4180–4188, doi:10.1002/2016GL068896.

Oke, A. M. C., N. J. Tapper, and D. Dunkerley (2007), Australian landscape: The role of key meteorological variables and surface conditions in defining frequency and spatial characteristics, *J. Arid. Environ.*, *71*(2), 201–215.

Onishchenko, O., O. Pokhotelov, and V. Fedun (2013), Convective cells of internal gravity waves in the Earth's atmosphere with finite temperature gradient, *Ann. Geophys.*, *31*, 459–462.

Onishchenko, O., W. Horton, O. Pokhotelov, and L. Stenflo (2014), Dust devil generation, *Phys. Scr.*, *075606*(7).

Onishchenko, O., O. Pokhotelov, W. Horton, and V. Fedun (2015), Dust devil vortex generation from convective cells, *Ann. Geophys.*, *33*(11), 1343–1347.

Rennó, N. O., and H. B. Bluestein (2001), A simple theory for waterspouts, *J. Atmos. Sci.*, *58*, 927–932.

Rennó, N. O., M. L. Burkett, and M. P. Larkin (1998), A simple thermodynamic theory for dust devils, *J. Atmos. Sci.*, *55*, 3244–3252.

Ringrose, T. J. (2005), Dust devils: Inside dust devils, *Astron. Geophys.*, *46*(12), 5.16–5.19.

Ryan, J. A., and J. J. Carroll (1970), Dust devil wind velocities: Mature state, *J. Geophys. Res.*, *75*(3), 531–541.

Shukla, P. K., and L. Stenflo (2012), Acoustic gravity tornadoes in the atmosphere, *Phys. Scr.*, *86*(6), 065403.

Stenflo, L. (1996), Nonlinear equations for acoustic gravity waves, *Phys. Lett. A*, *222*(6), 378–380.

Sinclair, P. C. (1973), The lower structure of dust devils, *J. Atmos. Sci.*, *30*, 1599–1619.

Thomas, P., and P. J. Gierasch (1985), Dust devils on Mars, *Science*, *230*, 175–177.